Sequence Specificity and Role of Proximal Amino Acids of the Histone H3 Tail on Catalysis of Murine G9a Lysine 9 Histone H3 Methyltransferase

Hang Gyeong Chin, Mihika Pradhan, Pierre-Olivier Estève, Debasis Patnaik, Thomas C. Evans, Jr., and Sriharsa Pradhan*

New England Biolabs, 240 County Road, Ipswich, Massachusetts 01938-2723

Received May 26, 2005; Revised Manuscript Received August 2, 2005

ABSTRACT: The activity of recombinant murine G9a toward lysine 9 of histone H3 was investigated. GST fusion proteins containing various lengths of the histone H3 amino-terminal tail were used as substrates in the presence of recombinant G9a enzyme and AdoMet cosubstrate. The minimal substrate methylated by G9a contained seven amino acids (TARKSTG) of the histone H3 tail. Furthermore, mutational analysis of the minimal substrate was performed to identify the amino acids essential for G9a-mediated methylation. All amino acids except Thr-11 were indispensable for the methylation reaction. Steady-state kinetic analysis of the wild-type and histone H3 point mutants, lysine 4 changed to alanine (K4A) or lysine 27 changed to alanine (K27A), with purified G9a revealed similar catalytic efficiency but a reduction in turnover number (k_{cat}) from 78 to 58 h^{-1}. G9a methylated synthetic peptide substrates containing the first 13 amino acids of histone H3 efficiently, although methylation, acetylation, or mutation of proximal Lys-4 amino acids reduced Lys-9 methylation. The k_{cat} for wild-type peptide substrate vs Lys-4 acetyl- or trimethyl-modified peptide were 88 and 32 h^{-1}, respectively, and the K_m for the peptides varied from 0.6 to 2.2 μM, resulting in a large difference (15−91) in catalytic efficiency. Ser-10 or Thr-11 phosphorylation resulted in poor methylation by G9a. Immunoprecipitation of unmodified and Ser-10 and Thr-11 phosphorylated histone H3 displayed mostly Lys-4 dimethylation. Dimethylated Lys-9 was reduced in Ser-10 and Thr-11 immunoprecipitated phosphorylated histones as compared to nonphosphorylated H3. In an immunocytochemical assay, GFP fusion SUV39H1 or G9a did not colocalize with phosphorylated histone H3. Thus, Ser-10/Thr-11 phosphorylation impairs Lys-9 methylation. These data suggest that the sequence context of the modified residue affects G9a activity and the modification in the proximal amino acids influences methylation.

In eukaryotes the genome is packaged with histone octamers into chromatin resulting in several thousand fold compaction of the genomic DNA. The basic unit of chromatin is nucleosomes, typically composed of two copies of histone H2A, H2B, H3, and H4, an octamer, and 146 base pairs of double-stranded DNA. Each histone molecule contains a structured core domain and an unstructured amino-terminal tail of about 25−40 amino acids (*1*). The amino terminus of histones undergoes diverse posttranslational modifications such as acetylation, methylation, phosphorylation, ubiquitination, and ADP-ribosylation (*2*). It is becoming increasingly apparent that such modifications determine the interaction of regulatory and structural proteins that may in turn regulate chromatin structure. Regulation of chromatin structure is vital for cell survival since essential cellular processes such as DNA replication, repair, and transcription require dynamic chromatin changes (*3*). Acetylation and methylation of arginine have been linked mainly with transcriptional stimulation (*4*), and phosphorylation of serine acts as a signal for dynamic chromatin condensation and decondensation during the cell cycle (*5*).

The ability of lysine residues to be mono-, di-, or trimethylated adds significant complexity to the posttranslational status of histone H3 and H4 (*6*, *7*). Furthermore, there are at least eight lysine residues (K4, K9, K14, K23, K27, K36, K37, and K79) and four arginine residues (R2, R17, R26, and R128) in histone H3 that are methylated (*8*). Methylation of R17 in histone H3 is found to be associated with hormone-responsive promoters after induction. Coactivator-associated arginine methyltransferase (CARM1) can methylate R17 and R26 residues in vitro and act synergistically with other coactivators, such as acetyltransferases p300 and PCAF, suggesting that arginine methylation and histone acetylation are associated with transcriptional activation (*9*). Indeed, after hormone induction, methylation of R17 and acetylation of K18 and K23 of histone H3 were observed in the presenilin promoter. Increased methylation by CARM1 on preacetylated histone H3 as compared to nonacetylated substrate suggested that acetylation might increase the substrate affinity of the enzyme. Similar to histone H3, histone H4, H2B, and H2A also exhibit various degrees of lysine and arginine methylation.

Several other fully activated promoters display trimethylated Lys-4 in histone H3 (*10*) although basal expression levels from the promoters correlated with dimethylated Lys-4 in histone H3. This suggests that di- to trimethylation of

* Corresponding author. Tel: (978) 380-7227. Fax: (978) 921-1350. E-mail: pradhan@neb.com.

10.1021/bi0509907 CCC: $30.25
Published on Web 09/07/2005

Lys-4 may increase the efficiency of nucleosome remodeling and transcriptional reinitiation by generating more favorable recognition sites for corresponding transcription factors. A recent survey of human chromosome 21 and 22 for histone H3 lysine di- and trimethylation at position 4 showed the correlation of trimethylation with transcriptional starts, while dimethylation occurred elsewhere in the vicinity of the transcriptionally active genes (*11*). Contrary to methylation of Lys-4, Lys-9 methylation in histone H3 is present mainly in silenced chromatin regions known as heterochromatin (*12*). The pericentric heterochromatin region of the nucleus is enriched with heterochromatin binding protein HP1 that binds to methylated histone H3. Along with HP1 protein, lysine 9 histone H3 methyltransferases are also found in this region. The Suv39h class of enzymes in mammals (*12*), Clr4 in yeast (*13*), and Su(var)3-9 families in *Drosophila* (*14*) often play a dominant role in establishing and maintaining heterochromatin via methylation of Lys-9 in histone H3. Furthermore, deletion of Suv39h1 in murine embryonic stem cells reduced histone H3 trimethylation significantly (*15*).

In the nonheterochromatic loci, lysine 9 methylation is maintained by another SET domain containing enzyme, G9a (*16*). G9a is 1263 amino acids, and the methyltransferase activity is located at the carboxy terminus. This enzyme is about 10−20-fold more active than the Suv39h1 class of enzymes on histone H3 substrates (data not shown). To study the catalytic activities of G9a in vivo, Tachibana et al. created G9a-deficient mice and embryonic stem cells (*17*). G9a null cells demonstrated a lack of histone H3 Lys-9 methylation in the euchromatic region. Lack of G9a either killed or deformed the mice and the cells, indicating that G9a is a dominant H3-K9 methyltransferase in vivo. It also suggests that G9a-mediated methylation of euchromatin is a key component of the mechanism that regulates gene expression during embryogenesis. More cells underwent apoptosis in G9a-deficient mice, and this seemed to be the main cause of deformed embryos. However, these embryos still possessed a significant amount of mitotic cells that displayed growth defects while undergoing cell differentiation but not during normal cellular functions. This suggests that G9a is not required for simple proliferating processes but is necessary for some important events during embryonic development. They also found that G9a exerts a transcriptionally suppressive functionality dependent on its histone methyltransferase activity.

There are a number of crystallographic data available on SET domain containing enzymes (*18*−*21*). Product specificity and structural analysis of *Neurospora crassa* histone H3 methyltransferase, DIM5, have been studied in detail (*22*). Similarly, kinetic mechanisms and mutational effects of the SET domain on catalysis and substrate choice of G9a have been well studied (*23*−*25*). However, little is known about the amino acids involved at the substrate level for sequence specificity and steady-state kinetic properties in the presence of a modified amino acid. Thus, an attempt was made to determine the minimal length of the amino acid substrate needed for G9a activity. The crucial amino acids were determined by mutational analysis of the minimal substrate. Furthermore, results of mutation or modifications of Lys-4 by acetylation or methylation and phosphorylation of adjacent serine/threonine residues on G9a-mediated methylation of Lys-9 were investigated herein.

MATERIALS AND METHODS

GST Fusion Constructs and Protein Purification. Chemically synthesized DNAs [New England Biolabs (NEB)] were dissolved in sterile Tris−EDTA buffer (10 mM Tris-HCl and 1 mM EDTA, pH 8.0). Equal amounts of each oligonucleotide were mixed in the presence of DNA annealing buffer (50 mM Tris-HCl, pH 7.4, 1 mM Na_2EDTA, and 100 mM NaCl). The solution was heated at 99 °C for 2 min, 65 °C for 10 min, 42 °C for 10 min, and 37 °C for 10 min to facilitate annealing to give rise to a double-stranded DNA. For GST-H3[1] (1−13): top strand, AATTCGCACGAACAAAGCAAACAGCTCGTAAGTCCACTGGAGGTG; bottom strand, TCGACACCTCCAGTGGACTTACGAGCTGTTTGTTCTGTTCGTGCG. For GST-H3 (3−13): top strand, AATTCACAAAGCAAACAGCTCGTAAGTCCACTGGAGGTG; bottom strand, TCGACACCTCCAGTGGACTTACGAGCTGTTTGTTCTGTG. For GST-H3 (5−13): top strand, AATTCCAAACAGCTCGTAAGTCCACTGGAGGTG; bottom strand, TCGACACCTCCAGTGGACTTACGAGCTGTTTGG. For GST-H3 (6−12): top strand, AATTCACAGCTCGTAAGTCCACTGGAG; bottom strand, TCGACTCCAGTGGACTTACGAGCTGTG. For GST-H3 (6−11): top strand, AATTCGCTCGTAAGTCCACTG; bottom strand, TCGACAGTGGACTTACGAGCG.

To generate point mutation, the following oligonucleotides were chosen for the GST fusion construct. For GST-H3 (T6A): top strand, AATTCGCTGCTCGTAAGTCCACTGGAG; bottom strand, TCGACTCCAGTGGACTTACGAGCAGCG. For GST-H3 (R8A): top strand, AATTCACAGCTGCTAAGTCCACTGGAG; bottom strand, TCGACTCCAGTGGACTTAGCAGCTGTG. For GST-H3 (K9A): top strand, AATTCACAGCTCGTGCTTCCACTGGAG; bottom strand, TCGACTCCAGTGGAAGCACGAGCTGTG. For GST-H3 (S10A): top strand, AATTCACAGCTCGTAAGGCTACTGGAG; bottom strand, TCGACTCCAGTAGCCTTACGAGCTGTG. For GST-H3 (T11A): top strand, AATTCACAGCTCGTAAGTCCGCTGGAG; bottom strand, TCGACTCCAGCGGACTTACGAGCTGTG. For GST-H3 (G12A): top strand, AATTCACAGCTCGTAAGTCCACTGCTG; bottom strand, TCGACAGCAGTGGACTTACGAGCTGTG. These were made and annealed to double-stranded DNA. The mutations are shown in parentheses, and mutant triplet codons are underlined.

For cloning into pGEX 5.1 (Amerhsan Pharmacia), the plasmid was digested with *Eco*RI and *Sal*I (NEB) and ligated with the annealed DNA in the presence of T4 DNA ligase and T4 polynucleotide kinase (NEB). All of the recombinant clones were sequenced for validation of insert and mutation.

The recombinant clones were transformed into *Escherichia coli* ER2566 (NEB), and protein expression was induced with 0.5 mM IPTG for 4 h at 37 °C. The *E. coli* pellets were stored at −20 °C overnight. The cell pellet was resuspended in 1× phosphate buffer, 0.5% (v/v) Triton X-100, and 0.2 mL of PMSF (7 mg/mL). Cells were sonicated at 50% duty cycle using a microtip at max using the pulse mode for 30 s. Lysed cells were mixed for 15 min on ice and centrifuged at 10000 rpm for 1 h at 4 °C. The supernatant was collected and mixed with gluthatione−Sepharose 4B (Amersham

[1] Abbreviations: AdoMet, *S*-adenosyl-L-methionine; GST, glutathione *S*-transferase; wt, wild type; IP, immunoprecipitation.

Table 1: Peptide Substrates Used in Kinetic Analysis of Recombinant G9a[a]

peptide sequence	peptide name
CARTKQTARKSTGGKAPRK-BT	wt-H3
CARTAQTARKSTGGY-BT	K4AK9
CART(K-acetyl)QTARASTGGY	K4-acetylK9
CART(K-trimethyl)QTARASTGGY	K4-trimethylK9
CARTKQTARKSTGG	wt-H3 (1−13)
CARTKQTARK(S-phos)TGG	wt-H3 (S10phos)
CARTAQTARS(T-phos)GGY	wt-H3 (T11phos)

[a] Abbreviations: BT (biotin), S10phos (serine 10 phosphorylated), and T11phos (threonine 11 phosphorylated).

Pharmacia) for 1 h at 4 °C. The beads were centrifuged at 1300 rpm for 5 min and resuspended three times with 5 mL of 1× PBS plus 0.5% (v/v) Triton X-100. The GST fusions bound to beads were stored at 4 °C.

Histone Methyltransferase Reaction, Filter Binding Assay, and Data Analysis. A typical histone methyltransferase assay contained a fixed amount of peptides representing the H3 tail or intact histone molecules, 10× G9a reaction buffer, 5 μM *S*-adenosyl-L-[*methyl*-^{3}H]methionine (Amersham Pharmacia), and 25 nM recombinant G9a. All reactions were performed at room temperature for 3 min at a final volume of 25 μL. Ten microliters of the reaction was spotted on P81 circles (Whatman). All filters were processed as per Patnaik et al. (*23*). Radioactive incorporation in cpm was measured and corrected for counting efficiency. Data were plotted using Prism4b (GraphPad Software Inc.). Peptides used for the in vitro histone methyltransferase assay were chemically synthesized and purified at NEB. Peptides used for assay are listed in Table 1.

Fluorography. After the methylation reaction the reaction mixture was separated on a SDS−polyacrylamide gel, stained with Coomassie brilliant blue, and further destained for detection of fusion proteins and enzyme. For each fluorography, 50 mL of EN^{3}HANCE solution (New England Nuclear) was added to the destained gel and kept on a shaker in a chemical hood for 1 h. After 1 h the EN^{3}HANCE solution was discarded, and 100 mL of cold MilliQ water was added to the gel. The gel was kept on a shaker for 30 min. The gel was dried between two cellophane films and exposed to Kodak Biomax MR X-ray film overnight at −80 °C. The film was processed after 12−24 h of exposure.

Immunoprecipitation and Western Blot Analysis. Core histones were solubilized and extracted by treating HeLa cell nuclei with 0.1 M H_2SO_4 and ethanol precipitated overnight. Histones were dissolved in 1× PBS, and 1 μg of specific antibodies was added and incubated overnight at 4 °C. Ten microliters of protein G−agarose was added and mixed for 2 h at 4 °C to capture the complex. Complexes were separated on a SDS gel, western blotted, and detected with specific antibodies.

GFP Fusion Constructs and Immunocytochemistry. G9a and SUV39H1 genes were PCR amplified and cloned into the pEGFPc2 vector (Clontech) to give rise to GFP-G9a and GFP-SUV39H1. These clones were transfected into HeLa cells (ATCC no. CCL-2). Transfected cells were fixed and immunostained with anti-Ser-10 or Thr-11 phosphospecific antibodies (Upstate). The slides were processed as per Esteve et al. (*25*) and visualized with a Zeiss 200M fluorescent microscope at 488 nm for GFP-SUV39H1 and GFP-G9a and at 568 nm for Alexa594-conjugated IgG secondary antibodies (Molecular Probes) for phosphorylated Thr-11/Ser-10 histone H3 detection (*26*). The nuclear staining by Hoechst 33342 was observed at 460 nm.

RESULTS

Minimal Substrate Length Determination for G9a. pGEX constructs with various histone H3 tail lengths were transformed into *E. coli* cells (Figure 1A). All fusion proteins were of >90% purity and were stable at 4 °C for several months. The GST fusion proteins were used as substrate molecules to determine which fusion could be utilized as a G9a substrate with radioactive AdoMet cofactor and independent of the rH3 globular domain. Upon methylation the protein substrate will acquire a tritiated methyl group that can be identified by fluorography. In the H3 tail GST fusion construct, we have used the wild-type H3 tail containing 1−13 amino acids [GST H3 (1−13)] as the starting substrate, since this substrate displayed a similar turnover number as that of rH3 molecules (Tables 2 and 4). Other fusion constructs used in the methylation assay have two [GST H3 (3−13)], four [GST H3 (5−13)], six [GST H3 (6−12)], and seven [GST H3 (6−11)] amino acids deleted. Indeed, the radioactive substrates [GST H3 (1−13)], [GST H3 (3−13)], [GST H3 (5−13)], and [GST H3 (6−12)] displayed a dark band on the X-ray film and, therefore, were methylated by G9a (Figure 1B). The intensity of the dark bands decreased gradually from GST-H3 (1−13) to GST-H3 (6−12), suggesting that loss of proximal amino acids reduces the methylation reaction. Out of all the fragments that were methylated, the smallest was GST-H3 (6−12) containing amino acids TARKSTG in the fusion.

To determine which amino acids are essential for G9a-mediated methylation, a series of point mutations were made to the substrate GST-H3 (6−12) to create six constructs, GST-H3 (T6A), GST-H3 (R8A), GST-H3 (K9A), GST-H3 (S10A), GST-H3 (T11A), and GST-H3 (G12A) (Figure 1C). These substrates were then used in a methylation reaction, separated on a denaturing SDS−PAGE gel (Figure 1D, upper panel), and then fluorographed. None of the mutated substrates were methylated except GST-H3 (T11A). Indeed, GST-H3 (T11A) and GST-H3 (6−12), its wild-type fusion, displayed similar methylation as determined by the intensity of the radioactive band in fluorography, suggesting that mutation of threonine to alanine had no effect on G9a-mediated methylation (Figure 1D) while all other amino acids in the minimal substrate GST-H3 (6−12) are important for substrate specificity.

Steady-State Kinetic Properties of Recombinant G9a on rH3 and Its Mutant. To understand the effect of mutation in the unstructured tail of histone H3, recombinant histone H3 containing Lys-4 modified to Ala (H3(K4A)) and Lys-27 modified to Ala (H3(K27A)) was purified from *E. coli* (Figure 2A) and used as substrate with recombinant G9a. These two amino acids were chosen for point mutation because Lys-4 and Lys-27 methylation is associated with transcriptional regulation. By studying the G9a-catalyzed reaction at steady state, one can obtain essential kinetic parameters for a set of different substrates for comparison. We assumed that mutation in the unstructured amino-terminal tail of histone H3 does not affect the central globular domain.

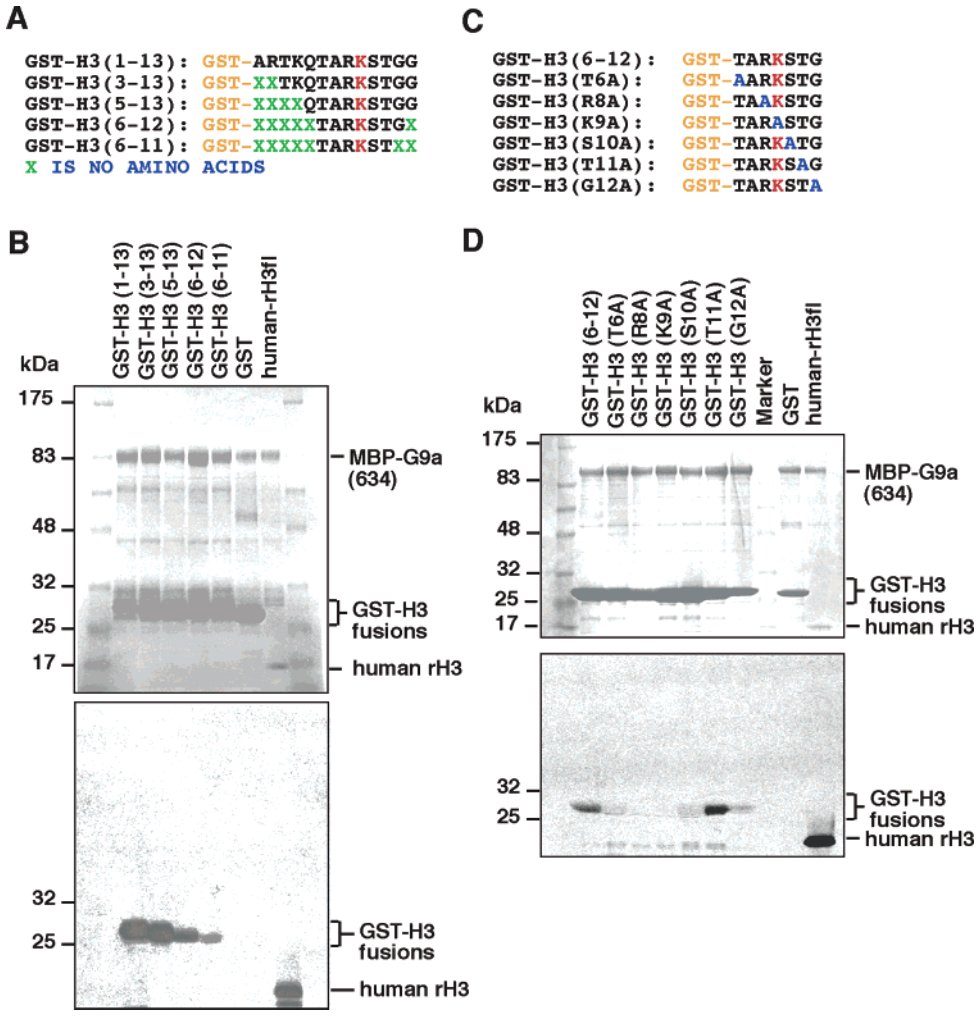

FIGURE 1: Minimal substrate length and sequence specificity of recombinant G9a. (A) Schematic diagram of GST fusion histone H3 amino-terminal tail proteins used in the study. Numbers in parentheses indicate the amino acid number of histone H3 that is fused to the GST protein. X shows the deleted amino acid(s) in the construct. (B) Minimal substrate length determination by in vitro methylation, followed by SDS−PAGE separation and Coomassie staining of the gel (top panel) and fluorography of the same gel (bottom panel). GST fusions, G9a, and human rH3 full-length histone proteins are indicated at the right and molecular mass at the left. (C) Point mutant minimal GST fusion substrates used for the study. The mutations are indicated in parentheses. (D) Determination of the role of amino acids in the minimal substrate for the G9a-mediated methylation reaction. The top panel shows the reaction products separated on a denaturing gel, and stained proteins are indicated at the right. In the bottom panel the fluorography of the same gel is shown. In (B) and (D) the fusion constructs used are indicated on the top.

Various amounts of wild-type and mutant histone H3's with saturating amounts of AdoMet cosubstrate along with a constant amount of full-length baculovirus-expressed G9a were incubated, and methylation was measured by filter binding assay. As the substrate concentration increased, the product accumulated, resulting in a hyperbolic curve. Michaelis−Menten plots for reaction velocity as a function of rH3 and rH3 (K4A) concentration (Figure 2B) are shown. A similar experiment was also performed with rH3 and rH3 (K27A) and shown in Figure 2C. Methylation saturation was observed for rH3 and its mutants at a substrate concentration of ~1.0 μM. The kinetic parameters with these substrates were obtained after nonlinear regression curve fit analysis of the product formation curve to determine essential steady-state kinetic parameters such as V_{max} and K_m. From the V_{max} values for each substrate, their k_{cat} was calculated and catalytic efficiency was determined. Kinetic parameters for rH3 and its mutants are shown in Table 2. The kinetic parameters for the rH3 substrate were very similar to our previous studies (*23*) with k_{cat} 78 h^{-1} and K_m ~0.26 μM. The K_m values for rH3 (K4A) and rH3 (K27A) were 0.23 and 0.17 μM, respectively, with a reduced catalytic turnover number of 58 h^{-1}. The catalytic efficiency posted for rH3 and its mutants remained the same. Thus, the mutation of the amino-terminal tail affects catalysis by recombinant murine G9a.

Influence of Modified or Mutated Lys-4 and Phosphorylation of Ser-10 and Thr-11 on G9a-Mediated Methylation on H3-Lys-9. Since mutation of K4A in histone H3 affected catalysis, we investigated if modification of K4 by acetylation or methylation will have any effect on G9a catalysis. To perform this experiment, a series of chemically synthesized peptides were used (Table 1). Indeed, mutation of K4A or modification of K4 to the acetylated or trimethylated form reduced the turnover numbers of the substrates as compared to the wild type (Figure 3A,B). The Lys-4 acetylated peptide displayed a higher K_m value of 2.2 μM as compared to 0.9 μM for the wild-type peptide along with a 6-fold difference in catalytic efficiency between them (Table 3). This suggests that acetylation of Lys-4 makes the substrate binding more

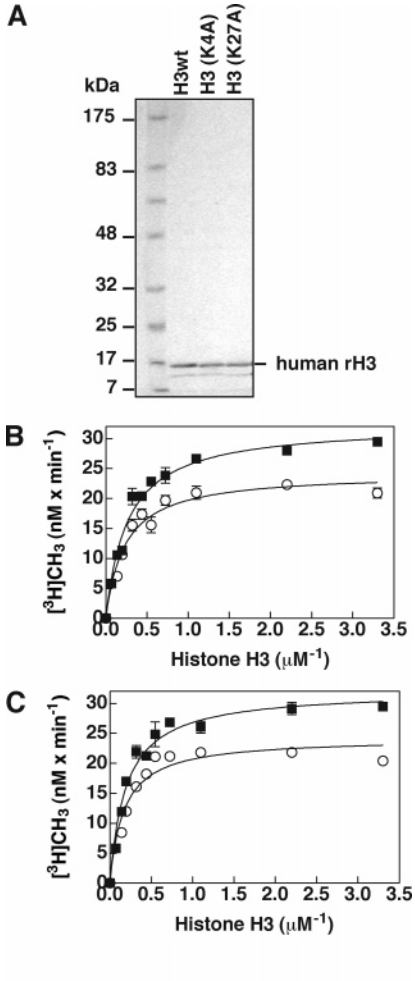

FIGURE 2: Purification of recombinant histone H3 and its mutants along with their substrate−velocity curves. (A) Single-column purification and denaturing gel electrophoresis of recombinant histone H3 wild type (H3wt) and its mutants H3 (K4A) and H3 (K27A) as indicated. In both H3 (K4A) and H3 (K27A) lysine 4 or 27 is mutated to alanine. Molecular mass (in kDa) is indicated on the left, and human recombinant histones are shown at the right. (B) Full-length G9a activity with different concentrations of H3wt (filled squares) or H3 (K4A) (open circles). The concentrations of the substrate were 0.07, 0.14, 0.2, 0.32, 0.44, 0.55, 0.726, 1.1, 2.2, and 3.3 μM. The reactions were performed with a fixed concentration of G9a enzyme (25 nM) and AdoMet (5 μM). Product formation was plotted versus substrate concentration, and nonlinear regression was performed to determine the K_m^{H3} values of the substrate. (C) Similar substrate−velocity curve to that of (B), except the velocity of the reaction, as determined by product formation, is shown for H3wt (filled squares) and H3 (K27A) (open circles). The concentrations of the substrates remained the same as that of (B) for comparison.

Table 2: Comparison of Steady-State Kinetic Parameters of Recombinant G9afl on Recombinant Wild-Type and Mutant Histone H3 Substrates

substrate[a]	k_{cat} (h^{-1})	K_m^{H3} (μM)	k_{cat}/K_m^{H3} ($\times 10^6$ M^{-1} h^{-1})
rH3	78 ± 2	0.26 ± 0.02	300
rH3(K4A)	58 ± 2	0.23 ± 0.03	253
rH3(K27A)	58 ± 2	0.17 ± 0.03	341

[a] The mutation in the recombinant full-length histone H3 is in parentheses.

difficult, whereas methylation of Lys-4 does not change binding, and both modifications affect catalysis of Lys-9

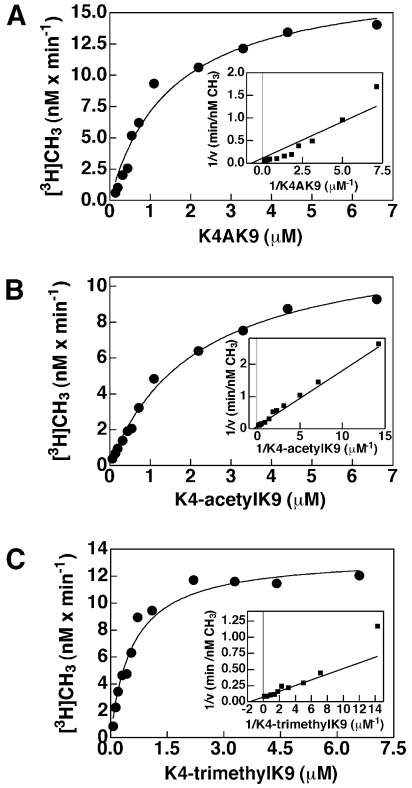

FIGURE 3: Substrate−velocity curves and double reciprocal plots of the initial velocity versus substrate concentration. (A) Full-length recombinant G9a activity with lysine 4 mutated to the alanine (K4AK9) peptide substrate. Methylation reactions were performed with substrate concentrations of 0.07, 0.14, 0.2, 0.32, 0.44, 0.55, 0.726, 1.1, 2.2, 3.3, 4.4, and 6.6 μM and fixed enzyme and AdoMet concentrations of 25 nM and 5 μM, respectively. Product formation was plotted versus substrate concentration, and nonlinear regression was performed to determine the K_m^{pep} values of the substrate. The insert shows the Lineweaver−Burk plot of the substrate velocity. V_{max} and K_m^{pep} were calculated from the substrate velocity plot. (B) A similar substrate velocity plot for the lysine 4 acetylated substrate (K4-acetylK9) along with a Lineweaver−Burk plot of the substrate velocity as an insert. The substrate concentrations were kept identical to K4AK9. (C) A similar substrate velocity plot for the lysine 4 trimethylated substrate (K4-trimethylK9) along with a Lineweaver−Burk plot of the substrate velocity as an insert. The substrate concentrations were kept identical to K4AK9 and K4-acetylK9 for comparison.

Table 3: Comparison of Steady-State Kinetic Parameters of Recombinant G9afl on Synthetic Peptide Substrates[a]

substrate	k_{cat} (h^{-1})	K_m^{pep} (μM)	k_{cat}/K_m^{H3} ($\times 10^6$ M^{-1} h^{-1})	ref
wt-H3	88 ± 4	0.9 ± 0.1	91	*34*
K4AK9	43 ± 2	1.5 ± 0.2	29	present work
K4-acetylK9	32 ± 1	2.2 ± 0.3	15	present work
K4-trimethylK9	32 ± 2	0.6 ± 0.03	53	present work

[a] Peptide nomenclature and modifications are presented under Experimental Procedures. wt-H3 indicates the first 19 amino acids of the amino terminus of histone H3.

(Figure 3C, Table 3). We further examined if phosphorylation can modulate G9a catalysis on Lys-9. There are two amino acids, Ser-10 and Thr-11, next to Lys-9 that can potentially be phosphorylated. Serine 10 phosphorylation is a marker for chromosome condensation during cell division and also participates in chromatin relaxation and gene expression during interphase. To study this effect, synthetic peptide

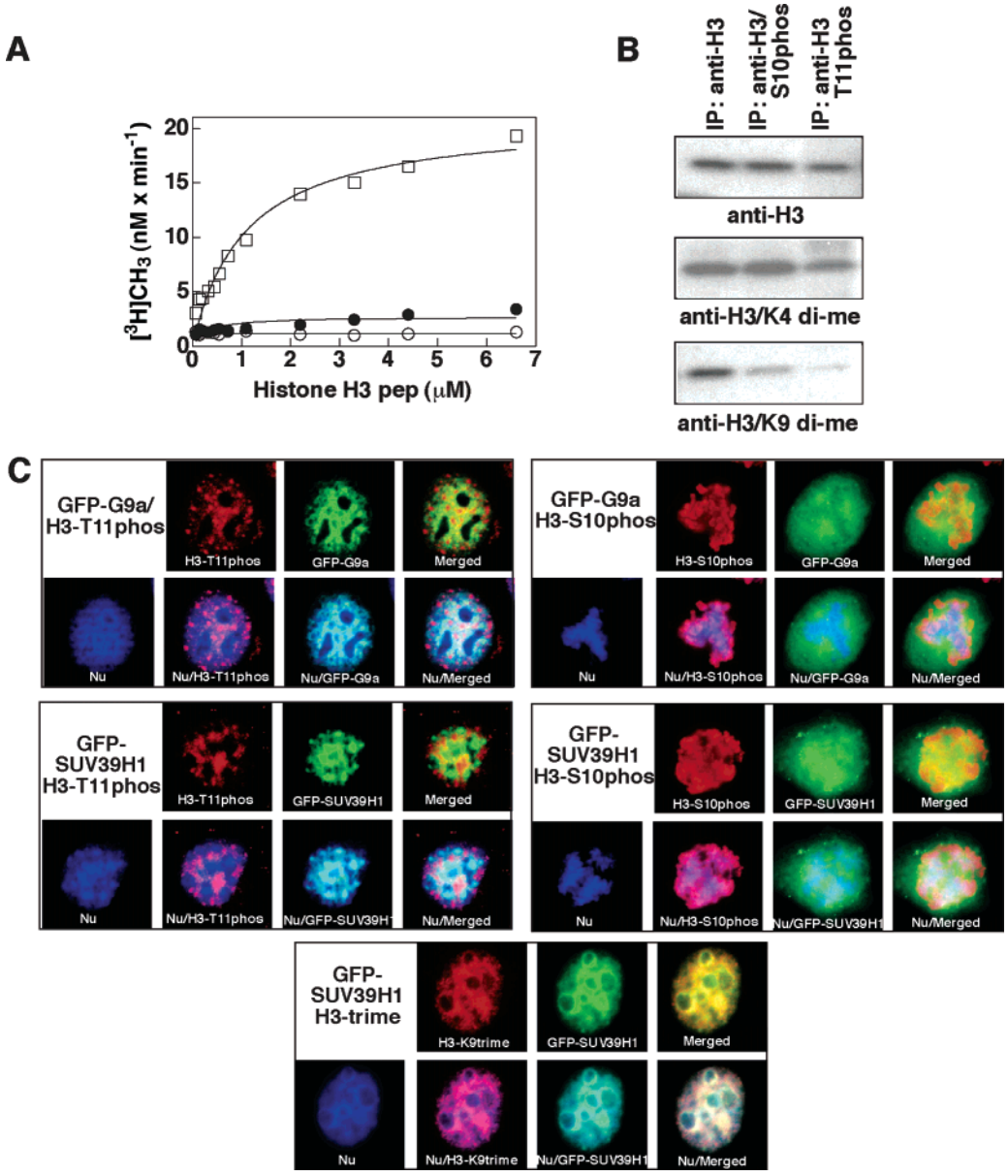

FIGURE 4: Phosphorylation of proximal amino acids impairs Lys-9 methylation and excludes histone H3 Lys-9 methyltransferase from binding. (A) Full-length G9a activity with different concentrations of peptide substrates: wt-H3 (1−13) as open squares, wt-H3 (T11phos) as filled circles, and wt-H3 (S10phos) as open circles. The concentrations of the substrate were 0.07, 0.14, 0.2, 0.32, 0.44, 0.55, 0.726, 1.1, 2.2, 3.3, 4.4, and 6.6 μM along with a fixed concentration of G9a enzyme (25 nM) and AdoMet (5 μM). (B) Determination of histone modification in immunoprecipitated histones from HeLa cells. Immunoprecipitated unmodified and modified histones H3 are indicated on the top along with antibodies to reveal the modifications below each western blot panel. Antibodies specific for phosphorylated serine 10 (anti-H3/S10phos), threonine 11 (anti-H3/T11phos), Lys-4 dimethylated (anti-H3/K4 di-me), and Lys-9 dimethylated (anti-H3/K9 di-me) are indicated. (C) Immunocytochemical localization of phosphorylated histones and histone Lys-9 methyltransferases. GFP fusion G9a and SUV39H1 are indicated as GFP-G9a and GFP-SUV39H1, respectively, and observed as green fusions in the indicated panels. The nucleus or condensed nuclear material (Nu) is shown. The phosphorylated and Lys-9 trimethylated histone H3s are shown as red.

substrates with either Ser-10 [wt-H3 (S10phos)] or Thr-11 [wt-H3 (T11phos)] were used for steady-state kinetic analysis (Figure 4A). Neither wt-H3 (T11phos) nor wt-H3 (S11phos) was a good substrate for the methylation reaction (Table 4). A 12−30-fold decrease in Lys-9 methylation was observed with wt-H3 (T11phos) and wt-H3 (S10phos) substrate, respectively, as determined by an in vitro assay demonstrating that G9a cannot methylate its target effectively if there is a phosphorylated amino acid next to it. To confirm this observation, in vivo immunoprecipitation assays were performed. HeLa core histone proteins were acid extracted and incubated with either anti-H3, anti-H3/S10phospho, or H3/T11phospho antibodies, and the immunoprecipitated fractions were examined by western blotting and probed with anti-H3/K4 dimethylated and anti-H3/Lys-9 dimethylated antibodies (Figure 4B). The aim of this immunoblot was to determine if Ser-10/Thr-11 phosphorylated histone would allow Lys-4 and Lys-9 methylation. Western blotting with anti-H3/Lys-4 dimethylated antibody showed strong bands in all of the immunoprecipitated samples, demonstrating that both Lys-4 methylation and Ser-10/Thr-11 phosphorylation can coexist on the same histone molecule. However, the same samples probed with antibody specific for dimethylated Lys-9 of histone H3 only cross-reacted strongly with histone molecules immunoprecipitated with anti-histone H3 but not with anti-H3/S10p and anti-H3/T11p, confirming enriched

Table 4: Comparison of Steady-State Kinetic Parameters of Recombinant G9afl on Synthetic Peptide Substrates with Proximal Phosphorylation[a]

substrate	k_{cat} (h^{-1})	K_m^{pep} (μM)	k_{cat}/K_m^{H3} ($\times 10^6$ M^{-1} h^{-1})
wt-H3 (1−13)	74 ± 2	1.1 ± 0.1	67
wt-H3 (T11phos)	18 ± 0.6	0.6 ± 0.16	30
wt-H3 (S10phos)	6.5 ± 0.6		

[a] Peptide nomenclature and modifications are presented under Experimental Procedures. All three peptides are 13 amino acids long each. The phosphorylation is shown in parentheses with the 10th serine and 11th tyrosine as S10phos and T11phos, respectively.

histone H3 with S10 and T11 phosphorylation have only a small amount of K9 methylation. Thus phosphorylation of either S10 or T11 in the proximity of K9 can impair its methylation by G9a both in vivo as well as in vitro.

We further examined the relationships between phosphorylated Ser-10 and Thr-11 histone H3 and G9a and SUV39H1 in vivo. Both G9a and SUV39H1 participate in Lys-9 methylation in the euchromatic and heterochromatic fraction of the genome (*12*, *16*), respectively. For a reaction to proceed, the enzyme must bind to the substrate for methyl group transfer. Thus, an enzyme and its substrate would be colocalized inside a cell. Chromatin immunoprecipitation experiments show binding of G9a to dimethylated Lys-9 histone H3 and SUV39H1 and its mouse homologue Suv39h1 to trimethylated Lys-9 histone H3, the product of the reaction. To determine the colocalization profile of G9a and SUV39H1, GFP fusion constructs, GFP-G9a or GFP-SUV39H1, were cotransfected into HeLa cells, followed by fixing and probing with Ser-10 phosphospecific or Thr-11 phosphospecific antibodies (Figure 4C). In HeLa cells Thr-11 phosphorylated histone H3 were distributed throughout the nucleus and were clearly enriched at specific regions as evidenced by its punctate staining patterns. Furthermore, Thr-11 phosphorylated histone H3's were excluded from nucleoli and the Hoechst-stained dense region of the nucleus that is associated with transcriptionally silent heterochromatin. Previous studies have identified these densely stained regions to be associated with trimethylated Lys-9 in histone H3 (*12*, *17*). Indeed GFP-SUV39H1 molecules were found to be associated with the Hoechst dense region of the chromatin to various extents (Figure 4C) and were poorly colocalized with Thr-11 phosphorylated histone H3. A similar experiment was performed with Ser-10 phosphospecific antibody and GFP-G9a and -SUV39H1 fusions. Since Ser-10 phosphorylation occurs during mitosis (*7*), HeLa cells transfected with GFP fusions and stained with Ser-10 phosphospecific antibodies were scored for mitotic cells. Indeed, the mitotic cells were enriched with Ser-10 phosphorylated histone H3, and they were predominately found on condensed chromatin. Once again, both GFP-G9a and GFP-SUV39H1 remained poorly associated with or excluded from the phosphorylated histone H3 and were found throughout the cell. These observations conclusively prove that phosphorylation of the proximal amino acids impairs Lys-9 methylation in the human cell via impairing enzyme−substrate interaction.

DISCUSSION

The mammalian genome is partitioned into euchromatin and heterochromatin on the basis of transcriptional permissiveness or repression. The transcriptionally active fractions are enriched with Lys-9 and Lys-27 mono- and dimethylated histone H3 molecules, whereas the constitutive heterochromatin is characterized by focal accumulation of Lys-9 trimethylated and Lys-27 monomethylated histone H3 (*15*). Furthermore, these heterochromatin regions lack Lys-4 mono- or dimethylated histone H3, a mark that is associated with an active promoter (*10*). Similarly, Lys-27 trimethylation is a prominent marker for the inactive X chromosome of the mammalian female species (*27*, *28*). A recent study in yeast chromatin showed a detailed boundary of various chromatin markers and transcriptional status of the genes (*11*). Furthermore, histone methyltransferase, G9a or SUV39H1, can mark distinctive methylation to defined distinct chromatin regions (*29*). Thus, epigenetic markers on the amino acids of histones participate in gene regulation. A family of SET domain containing enzymes establish these marks in mammalian cells (*30*). Often several enzymes methylate the same target amino acid residue. For example, Suv39h1, Suv39h2, G9a, EuHMT, and SetDB1 can methylate Lys-9 in histone H3. However, functional overlaps between different enzymes are not observed in vivo since genetic knockout of G9a or Suv39h1 in mice resulted in developmental abnormality such as severe growth retardation, chromosomal abnormality, and early lethality for G9a null animals (*12*, *17*, *31*). Thus, chromatin-specific epigenetic marks may be mediated by a different enzyme. Furthermore, histone modification enzymes such as G9a have stringent substrate specificity. Sharp catalytic reduction by G9a in response to the substrate length indicates that this enzyme needs a substrate of 7−10 amino acids. G9a also displayed a strong sequence specificity for methylation since mutation of any of the amino acids, with the exception of Thr-11, in the TARKSTG motif essentially inactivated the methylation reaction. These data fit well with the previous observations that G9a cannot effectively methylate Lys-27 of histone H3 despite the presence of a very similar ARKST motif (*24*).

Since several amino acids in the histone amino-terminal tail can be modified, each modification enzyme will face a different environment for catalysis as observed in this report. Methylation of Lys-4 in histone H3 may decrease the Lys-9 methylation reaction on the same molecule but will allow both a Lys-4 and Lys-9 methylation mark to coexist. The biological significance of this combination is yet to be established. It may be possible that activated chromatin displaying Lys-4 methylation may need Lys-9 methylation to occur for its regulation or Lys-9 methylation may act as an epigenetic mark for silencing a previously active chromatin, thus acting as an off switch via recruitment of G9a. A similar regulatory mechanism was also observed between Ser-10 or Thr-11 phosphorylation and Lys-9 methylation. Rea et al. observed mutual exclusiveness between S10 phosphorylation and Lys-9 methylation via an in vitro assay of a synthetic unmodified peptide in the presence of Ipl1/aurora kinase and murine Suv39h1, suggesting both phosphorylation as a transcriptional activation and methylation as a repression switch (*12*). Indeed, in our cytochemical observation neither G9a nor SUV39H1 were colocalized on the phosphorylated histone H3. Crystallographic structural information of target Lys-9 and DIM5, a *N. crassa* homologue of Suv39h1, shows a variety of interactions between the surrounding H3 sequences and amino acids L205 and

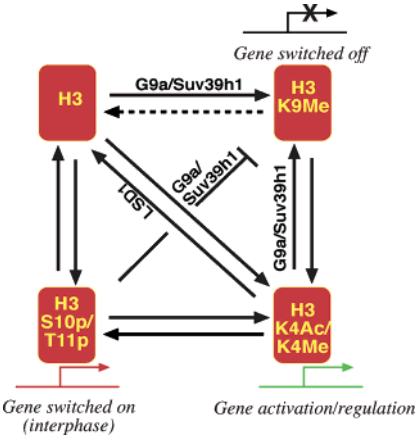

FIGURE 5: A model showing dynamics of gene expression correlated with histone H3 modification. Histone H3 unmodified (H3), acetylated at Lys-4 (H3K4Ac), and methylated at Lys-4 (H3K4Me) can be methylated at Lys-9 (H3K9Me) by G9a/SUV39H1 to bring on gene silencing. Histone H3 phosphorylation at Ser-10 (H3S10p) or Thr-11 (H3T11p) blocks binding of GFP-SUV39H1 or -G9a, thus impairing Lys-9 methylation mediated by G9a and SUV39H1. The transcriptional status of the chromatin-containing H3K4Me may be deregulated via demethylation mediated by LSD1 amine oxidase. The enzyme for Lys-9 demethylation is not known as shown by the dotted arrow. Thus the dynamics of gene expression via histone modification is dependent on a series of covalent modifications of the amino-terminal tail of histone H3 molecules.

A207 of the protein. Ser-10 hydrogen bonds with the backbone carbonyl of D209, and these interactions are critical for peptide recognition by DIM5. A negatively charged phosphate group on Ser-10 may disrupt the interaction between enzyme and substrate, thus leading to poor methylation (*22*). This mechanistic impairment of methylation of Lys-9 may occur in G9a because identical/similar amino acid residues L1138, D1140, and D1142 are also present in G9a. In a recent study, we have demonstrated that G9a-mediated methylation can occur without its amino-terminal region, suggesting that product specificity may only involve the carboxy terminus (*25*).

Thus, a proposed model for mammalian gene regulation may involve various dynamic states of the histone molecule. Various histone marks may participate in gene activation, repression, or rate modulation via Lys-4 acetylation or methylation, Ser-10 or Thr-11 phosphorylation, and Lys-9 methylation (Figure 5). The dynamic modification and gene regulation status was shown to involve G9a in sets of genes containing neuron responsive silencing elements (NRSE) via recruitment of neuron restrictive silencing element factor (NRSF) binding (*32*). A similar mechanism also operated for interferon-β gene transcriptional regulation by PRDI-BF1 recruitment of G9a to the promoter (*33*). Furthermore, histone modification, such as Lys-4 methylation that is linked to active transcription, may be regulated by the enzyme with amine oxidase function such as LSD1 (*34*). Thus, the dynamics of nuclear gene expression is a well-orchestrated event between several epigenetic modifiers and regulators.

ADDED IN PROOF

Following submission of our work, Metzger et al. (*35*) have demonstrated that LSD1 can demethylate methylated Lys-9 of histone H3 in andogen receptor target genes.

ACKNOWLEDGMENT

We thank Dr. D. G. Comb for encouragement and New England Biolabs, Inc., for support and assistance. This work is dedicated in the memory of Lipica Pradhan (1967−2005).

REFERENCES

1. Luger, K., Mader, A. W., Richmond, R. K., Sargent, D. F., and Richmond, T. J. (1997) Crystal structure of the nucleosome core particle at 2.8 Å resolution, *Nature 389*, 251−260.
2. Van Holde, K. E (1988) *Chromatin*, Springer-Verlag, New York.
3. Ehrenhofer-Murray, A. E. (2004) Chromatin dynamics at DNA replication, transcription and repair, *Eur. J. Biochem. 271*, 2335−2349.
4. Rice, J. C., and Allis, C. D. (2001) Histone methylation versus histone acetylation: new insights into epigenetic regulation, *Curr. Opin. Cell Biol. 13*, 263−273.
5. Prigent, C., and Dimitrov, S. (2003) Phosphorylation of serine 10 in histone H3, what for?, *J. Cell Sci. 116*, 3677−3685.
6. Jenuwein, T., and Allis, C. D. (2001) Translating the histone code, *Science 293*, 1074−1080.
7. Strahl, B. D., and Allis, C. D. (2000) The language of covalent histone modifications, *Nature 403*, 41−45.
8. Lachner, M., O'Sullivan, R. J., and Jenuwein, T. (2003) An epigenetic road map for histone lysine methylation, *J. Cell Sci. 116*, 2117−2124.
9. Xu, W., Cho, H., and Evans, R. M. (2003) Acetylation and methylation in nuclear receptor gene activation, *Methods Enzymol. 364*, 205−223.
10. Santos-Rosa, H., Schneider, R., Bannister, A. J., Sherriff, J., Bernstein, B. E., Emre, N. C., Schreiber, S. L., Mellor, J., and Kouzarides, T. (2002) Active genes are tri-methylated at K4 of histone H3, *Nature 419*, 407−411.
11. Bernstein, B. E., Kamal, M., Lindblad-Toh, K., Bekiranov, S., Bailey, D. K., Huebert, D. J., McMahon, S., Karlsson, E. K., Kulbokas, E. J., III, Gingeras, T. R., Schreiber, S. L., and Lander, E. S. (2005) Genomic maps and comparative analysis of histone modifications in human and mouse, *Cell 120*, 169−181.
12. Rea, S., Eisenhaber, F., O'Carroll, D., Strahl, B. D., Sun, Z. W., Schmid, M., Opravil, S., Mechtler, K., Ponting, C. P., Allis, C. D., and Jenuwein, T. (2000) Regulation of chromatin structure by site-specific histone H3 methyltransferases, *Nature 406*, 593−599.
13. Ivanova, A. V., Bonaduce, M. J., Ivanov, S. V., and Klar, A. J. (1998) The chromo and SET domains of the Clr4 protein are essential for silencing in fission yeast, *Nat. Genet. 19*, 192−195.
14. Schotta, G., Ebert, A., Krauss, V., Fischer, A., Hoffmann, J., Rea, S., Jenuwein, T., Dorn, R., and Reuter, G. (2002) Central role of *Drosophila* SU(VAR)3-9 in histone H3-K9 methylation and heterochromatic gene silencing, *EMBO J. 21*, 1121−1131.
15. Peters, A. H., Kubicek, S., Mechtler, K., O'Sullivan, R. J., Derijck, A. A., Perez-Burgos, L., Kohlmaier, A., Opravil, S., Tachibana, M., Shinkai, Y., Martens, J. H., and Jenuwein, T. (2003) Partitioning and plasticity of repressive histone methylation states in mammalian chromatin, *Mol. Cell 12*, 1577−1589.
16. Tachibana, M., Sugimoto, K., Fukushima, T., and Shinkai, Y. (2001) Set domain-containing protein, G9a, is a novel lysine-preferring mammalian histone methyltransferase with hyperactivity and specific selectivity to lysines 9 and 27 of histone H3, *J. Biol. Chem. 276*, 25309−25317.
17. Tachibana, M., Sugimoto, K., Nozaki, M., Ueda, J., Ohta, T., Ohki, M., Fukuda, M., Takeda, N., Niida, H., Kato, H., and Shinkai, Y. (2002) G9a histone methyltransferase plays a dominant role in euchromatic histone H3 lysine 9 methylation and is essential for early embryogenesis, *Genes Dev. 16*, 1779−1791.
18. Zhang, X., Tamaru, H., Khan, S. I., Horton, J. R., Keefe, L. J., Selker, E. U., and Cheng, X (2002) Structure of the Neurospora SET domain protein DIM-5, a histone H3 lysine methyltransferase, *Cell 111*, 117−127.
19. Min, J., Zhang, X., Cheng, X., Grewal, S. I., and Xu, R. M. (2002) Structure of the SET domain histone lysine methyltransferase Clr4, *Nat. Struct. Biol. 9*, 828−832.
20. Trievel, R. C., Beach, B. M., Dirk, L. M., Houtz, R. L., and Hurley, J. H. (2002) Structure and catalytic mechanism of a SET domain protein methyltransferase, *Cell 111*, 91−103.
21. Wilson, J. R., Jing, C., Walker, P. A., Martin, S. R., Howell, S. A, Blackburn, G. M., Gamblin, S. J., and Xiao, B. (2002) Crystal

structure and functional analysis of the histone methyltransferase SET7/9, *Cell 111*, 105−115.
22. Zhang, X., Yang, Z., Khan, S. I., Horton, J. R., Tamaru, H., Selker, E. U., and Cheng, X. (2003) Structural basis for the product specificity of histone lysine methyltransferases, *Mol. Cell 12*, 177−185.
23. Patnaik, D., Chin, H. G., Esteve, P. O., Benner, J., Jacobsen, S. E., and Pradhan, S. (2004) Substrate specificity and kinetic mechanism of mammalian G9a histone H3 methyltransferase, *J. Biol. Chem. 279*, 53248−53258.
24. Collins, R. E., Tachibana, M., Tamaru, H., Smith, K. M., Jia, D., Zhang, X., Selker, E. U., Shinkai, Y., and Cheng, X. (2005) In vitro and in vivo analyses of a Phe/Tyr switch controlling product specificity of histone lysine methyltransferases, *J. Biol. Chem. 280*, 5563−5570.
25. Estève, P. O, Patnaik, D., Chin, H. G., Benner, J., Teitell, M. A., and Pradhan, S. (2005) Functional analysis of the N- and C-terminus of mammalian G9a histone H3 methyltransferase, *Nucleic Acids Res. 33*, 3211−3223.
26. Estève, P. O., Chin, H. G., and Pradhan, S. (2005) Human maintenance DNA (cytosine-5)-methyltransferase and p53 modulate expression of p53-repressed promoters, *Proc. Natl. Acad. Sci. U.S.A. 102*, 1000−1005.
27. Silva, J., Mak, W., Zvetkova, I., Appanah, R., Nesterova, T. B., Webster, Z., Peters, A. H., Jenuwein, T., Otte, A. P., and Brockdorff, N. (2003) Establishment of histone h3 methylation on the inactive X chromosome requires transient recruitment of Eed-Enx1 polycomb group complexes, *Dev. Cell 4*, 481−495.
28. Plath, K., Talbot, D., Hamer, K. M., Otte, A. P., Yang, T. P., Jaenisch, R., and Panning, B. (2004) Developmentally regulated alterations in Polycomb repressive complex 1 proteins on the inactive X chromosome, *J. Cell Biol. 167*, 1025−1035.
29. Rice, J. C., Briggs, S. D., Ueberheide, B., Barber, C. M., Shabanowitz, J., Hunt, D. F., Shinkai, Y., and Allis, C. D. (2003) Histone methyltransferases direct different degrees of methylation to define distinct chromatin domains, *Mol. Cell 12*, 1591−1598.
30. Yeates, T. O. (2002) Structures of SET domain proteins: protein lysine methyltransferases make their mark, *Cell 111*, 5−7.
31. Peters, A. H., O'Carroll, D., Scherthan, H., Mechtler, K., Sauer, S., Schofer, C., Weipoltshammer, K., Pagani, M., Lachner, M., Kohlmaier, A., Opravil, S., Doyle, M., Sibilia, M., Jenuwein, T. (2001) Loss of the Suv39h histone methyltransferases impairs mammalian heterochromatin and genome stability, *Cell 107*, 323−337.
32. Roopra, A., Qazi, R., Schoenike, B., Daley, T. J., and Morrison, J. F. (2004) Localized domains of G9a-mediated histone methylation are required for silencing of neuronal genes, *Mol. Cell 14*, 727−738.
33. Gyory, I., Wu, J., Fejer, G., Seto, E., and Wright, K. L (2004) PRDI-BF1 recruits the histone H3 methyltransferase G9a in transcriptional silencing, *Nat. Immunol. 5*, 299−308.
34. Shi, Y., Lan, F., Matson, C., Mulligan, P., Whetstine, J. R., Cole, P. A., Casero, R. A., and Shi, Y. (2000) Histone demethylation mediated by the nuclear amine oxidase homolog LSD1, *Cell 119*, 941−953.
35. Metzger et al. (2005) *Nature* (Aug 3, Epub).

BI0509907